THE TDHF EVOLUTION OF COLLECTIVE MOTION IN HEAVY NUCLEI

J. Nemeth
Institute of Theoretical Physics, Eötvös University, Budapest, Hungary
and
S. Faidi and J.M. Irvine
Department of Theoretical Physics, The University, Manchester, M13 9PL, U.K.

INTRODUCTION

It is experimentally observed that excited states of compound nuclei in the rare earth and actinide regions produced in heavy ion reactions are more likely to decay by fission than states at a similar excitation energy produced in light ion reactions. The most probable explanation for this phenomena is that a much greater degree of collectivity of excitation is engendered by the heavy ions.

We have begun a programme to study the evolution of collective motion in heavy nuclei and in particular how this may be transferred to the fission mode within the framework of time-dependent Hartree-Fock theory. Some preliminary results are presented for ^{240}Pu and a 'model' rare earth nucleus ^{168}Gd.

THE TDHF CODE

In order to address the problem of the TDHF evolution of collective motion in heavy nuclei we have written two computer codes. Both contain the restriction of axial symmetry. The first is a static H.F. code with the facility to impose various constraints on the H.F. state via Lagrange multipliers, e.g. we could constrain various moments of the one-body density or a component of the angular momentum perpendicular to the symmetry axis. The second code uses the output from the static code as initial data for a TDHF calculation. The trigger for the time evolution can either be the relaxation of a static constraint or the superposition of a collective velocity field on the static configuration. For example, we could spin the H.F. state and watch its time evolution in the rotating frame, we could start it vibrating in various modes or we could initiate the time evolution with a combination of rotation and vibration.

The basic structure of the two codes is similar with the static code employing the imaginary time ansatz. The numerical techniques we have used are familiar from the works of Davies, Koonin and Feldmeier on axially symmetric rotating frame calculations and employs the Peaceman-Rachford method of approximating unitary operators. We shall, therefore, restrict ourselves to a brief review of the basic TDHF equations.

We approximate the true many-body wavefunction by a Slater determinant at each instant of time

$$\Psi(\underline{x}_1,\underline{x}_2 \ldots \underline{x}_A;t) = (A!)^{-\frac{1}{2}}\det \psi_i(\underline{x}_j,t) \tag{1}$$

where the single-particle states ψ_i are solutions of the TDHF equation

$$i\hbar\,\dot{\psi}_i(\underline{x},t) = \int d\underline{x}'\; h_{HF}(\underline{x},\underline{x}';t)\psi_i(\underline{x}',t) \tag{2}$$

As with most other TDHF calculations we have restricted ourselves to Skyrme interactions plus a direct Yukawa and Coulomb contribution thus reducing h_{HF} to a local operator

$$h^{\alpha}_{HF} = -\frac{\hbar^2}{2m}\nabla^2 + U^{\alpha}_s + U^{\alpha}_y + U^{\alpha}_c \tag{3}$$

where we have used

$$U^{\alpha}_s(x,t) = \tfrac{1}{2}t_0[(1+x_0/2)\rho(x,t) - (\tfrac{1}{2}+x_0)\rho_{\alpha}(x,t)]$$

$$+ \tfrac{1}{4}t_3[\rho^2(x,t) - \rho^2_{\alpha}(x,t)]$$

$$U^{\alpha}_y(\underline{x},t) = V_u\int d\underline{x}'\exp[-|\underline{x}-\underline{x}'|/a][|\underline{x}-\underline{x}'|]^{-1}a\rho(\underline{x},t)$$

$$+ (V_L - V_u)\int d\underline{x}'\exp[-|\underline{x}-\underline{x}'|/a][|\underline{x}-\underline{x}'|]^{-1}a\rho_{\alpha}(\underline{x}',t)$$

$$U^{\alpha}_c(\underline{x},t) = \delta_{\alpha,p}\, e^2\int d\underline{x}'[|\underline{x}-\underline{x}'|]^{-1}\rho_p(\underline{x}',t)\ .$$

Here $\rho(\underline{x},t)$ is the total one-body density

$$\rho(\underline{x},t) = \sum_{\alpha=n,p}\rho_{\alpha}(\underline{x},t) = \sum_{i=1}^{A}|\psi_i(\underline{x},t)|^2\ , \tag{4}$$

where the label α denotes neutrons n or protons p. The force parameters employed were

$t_0 = -497.66$ MeVfm^3 $\quad t_3 = 17288$ MeVfm^6 $\quad x_0 = 0.373$

$a = 2.175$ fm $\quad V_L = -55.25$ Mev $\quad V_u = -277.5$ MeV

With the restriction to axial symmetry and the use of cylindrical polar co-ordinates (r,z,θ) we may write

$$\psi_i(\underline{x},t) = \phi_i(r,z,t)\exp(in_i\theta) \tag{5}$$

where the component $n_i\hbar$ of angular momentum along the symmetry axis is conserved and the states n_i and $-n_i$ are degenerate. Thus in the absence of spin orbit forces

the single-particle level $|n_i|$ contains four nucleons $n_i \neq 0$ and two nucleons for $n_i = 0$.

If the single particle wavefunctions (5) are each multiplied by a phase factor $\exp[i\chi(\underline{x},t)]$ this corresponds to a collective velocity field

$$V_{col}(x,t) = \hbar \nabla\chi(\underline{x},t) \tag{6}$$

We have initiated TDHF evolution by vibrations

$$\chi_{vib} = \alpha (z - z_0)^2 \tag{7}$$

and rotations

$$\chi_{rot} = g(r,z,t)\cos\theta \quad . \tag{8}$$

We have considered only symmetric vibrations so that z_0 is the centre of mass of the nucleus. In the case of rotations the TDHF equations (2) may be written in the body fixed axially symmetric frame as

$$\begin{aligned} i\hbar\dot{\phi}_i &= -\hbar^2/2m\,[\frac{\partial^2}{\partial r^2} + \frac{1}{r}\frac{\partial}{\partial r} + \partial^2/\partial z^2 - n_i^2/r^2]\phi_i \\ &+ U_{HF}\,\phi_i + \hbar^2/2m \cdot \tfrac{1}{2}[(\partial g/\partial r)^2 + (\partial g/\partial z)^2 + (g/r)^2]\phi_i \\ &- \tfrac{1}{2}\hbar w\{z[(\partial g/\partial r) + g/r] - r\,\partial g/\partial z\}\phi_i \end{aligned} \tag{9}$$

where the phase function g is the solution of

$$\begin{aligned} &\partial\rho/\partial r\;\partial\tilde{g}/\partial r + \partial\rho/\partial z\;\partial\tilde{g}/\partial z + \rho\{\partial^2\tilde{g}/\partial r^2 + \frac{1}{r}\,\partial\tilde{g}/\partial r \\ &+ \frac{\partial^2\tilde{g}}{\partial z^2} - \frac{1}{r^2}\tilde{g}\} = \frac{m}{\hbar}\{z\frac{\partial\rho}{\partial r} - r\frac{\partial\rho}{\partial z}\} \end{aligned} \tag{10}$$

subject to the boundary conditions

$$\lim_{r\to\infty} \partial\tilde{g}/\partial r = mz/\hbar \;, \qquad \lim_{|z|\to\infty} \frac{\partial\tilde{g}}{\partial z} = -mr/\hbar \tag{11}$$

where $\tilde{g} = g/w$ and the rotational velocity w is determined by the conserved angular momentum about the y-axis

$$L_y = \hbar\int\rho\{z[\frac{\partial g}{\partial r} + g/r] - r\,\partial g/\partial z\}\pi r dr dz \tag{12}$$

An effective moment of inertia can then be defined by

$$\mathcal{J} = \hbar\int\rho\{z[\frac{\partial\tilde{g}}{\partial t} + \tilde{g}/r] - r\frac{\partial\tilde{g}}{\partial z}\}\pi r dr dz \tag{13}$$

so that the usual collective rotational energy is given by

$$E_{rot} = L_y^2/2\mathcal{J} \tag{14}$$

RESULTS

We first present the results of some preliminary studies on the nucleus ^{240}Pu. The valence neutron shell then consists of the N = 6 states while valence protons occupy states in the N = 5 shell. We are then faced with the choice of a number of static H.F. configurations depending on the occupancies of the valence orbits. We have chosen to consider the three configurations indicated in figure 1: The state S1 is the most stable H.F. configuration of valence protons in N = 5 levels and valence neutrons in N = 6 levels. This H.F. ground state lies within 1% of the experimental binding energy of ^{240}Pu indicating that our choice of force parameters is not unreasonable. The static H.F. configuration is then put in a rotating frame and the state of 35 units of angular momentum is generated. This lies at the exceptionally high excitation energy of 288 MeV. Next we searched on static H.F. configurations to find the state S2 which supports the H.F. Yrast state of 35ħ. S2 lies at an excitation energy of 30 MeV with respect to S1 but the 35ħ state which it supports lies at only 125 MeV excitation. Indeed the 55h state supported by S2 at an excitation energy of 256 MeV is still more bound than the 35ħ state based upon S1. Finally, we have constructed the static H.F. state S3 which maximises the elongation along the symmetry axis, this lies at 52 MeV with respect to S1 and supports a 35ħ level at 148 MeV excitation. We have used our TDHF code to follow the time evolution of the 35ħ states based upon S1, S2 and S3 and the 55ħ state based upon S2.

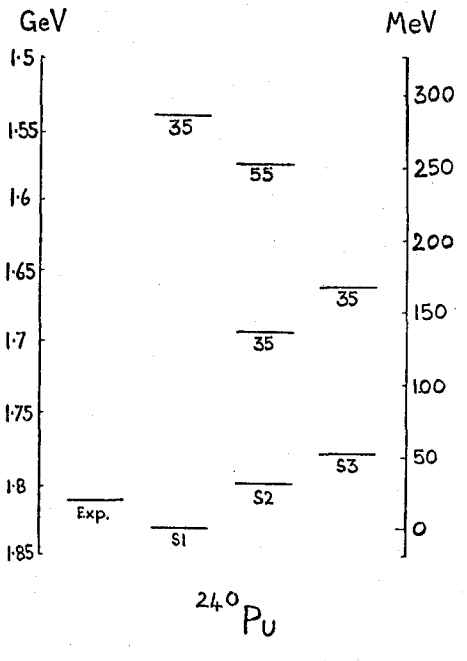

Figure 1

In figure 2 we show the time evolution of the one body density of the 35ħ state based upon S1 projected onto the z-axis, i.e. we plot $\int 2\pi r\rho(r,z,t)dr$. The time steps are in units of 10^{-21}s and the calculation is terminated at 0.5×10^{-21}s due to the appearance at the edge of our mesh, which is 58fm long, of detectable nuclear densities. This is traced to the emission of a few unbound nucleons from the nucleus. In figure 3 we plot the time evolution of $\langle z^2 \rangle$ and of the collective velocity of the right hand half of the one-body density in the z-direction V_c and

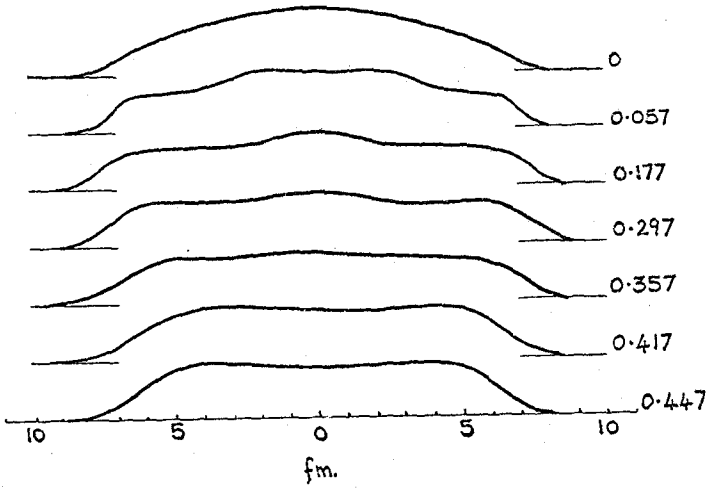

Figure 2

the quadrupole moment Q. We see that initially V_c increases rapidly as the nucleus elongates. V_c reaches a maximum and starts to decrease, it reaches zero when $\langle z^2 \rangle$ and $|Q|$ have reached their maximum values. As V_c becomes negative and the nucleus starts to retract $\langle z^2 \rangle$ and $|Q|$ begin to decrease.

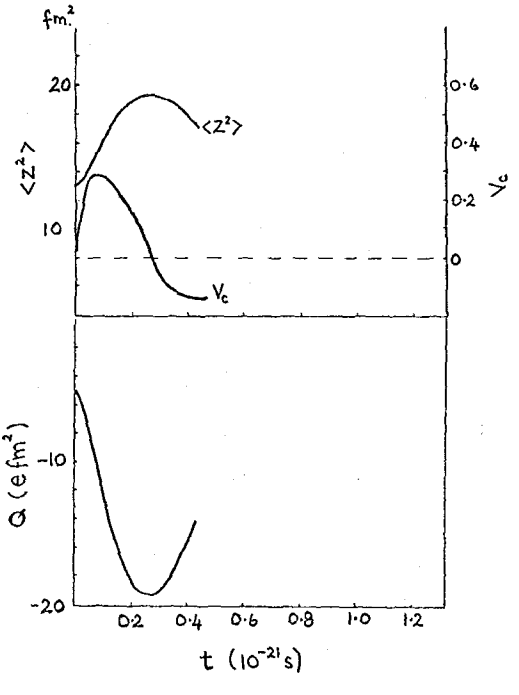

Figure 3

In figure 4 we show the time evolution of the one-body density for the 35ħ H.F. Yrast state. The structure of this state is completely different from that of the ground state. There is a large compact core to the nucleus with relatively low density highly extended arms which give it a large moment of inertia and hence a low rotational excitation energy. This configuration is so stable that the one-body density shows little change with time. Even at an angular momentum of 55ħ (figure 5) the same stability is exhibited although the arms are slightly more extended. In figure 6 we show the time evolution of $\langle z^2 \rangle$, V_c and Q for both the 35ħ (solid lines) and 55ħ (dashed lines) states. For the 35ħ state there is a hint of an oscillation in $\langle z^2 \rangle$ and Q, but following the initial stretching the amplitude of the second cycle is very small.

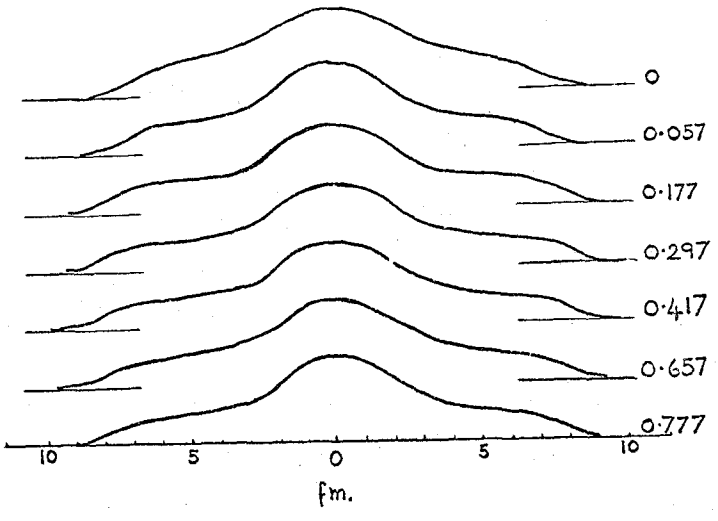

Figure 4

For the 55ħ state the initial stretching is greater and the amplitude of the second cycle is even smaller. The evolution of the 55ħ state is terminated at 0.6×10^{-21}s as unbound nucleons are again shaken off and reach the edge of the mesh.

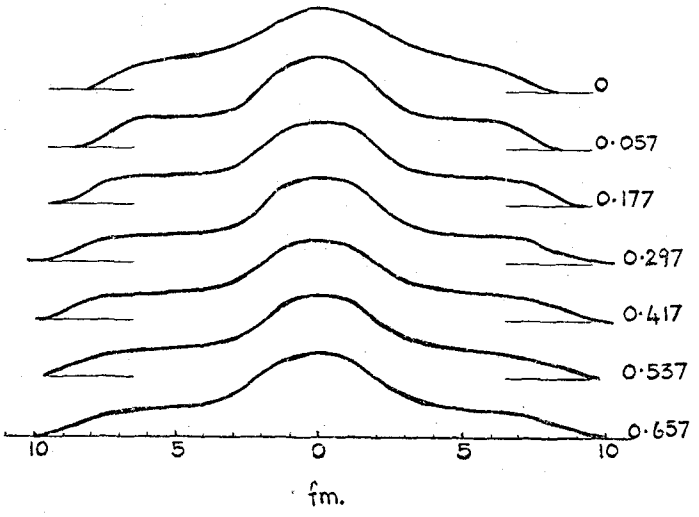

Figure 5

Finally, we consider the 35ħ state based upon S3, figures 7 and 8. Again we have a different intrinsic structure with a larger quadrupole moment and more of the bulk of the nucleus pushed away from the centre. This system exhibits a well defined highly damped oscillatory behaviour. It appears stable against particle emission but its behaviour is different from the other stable 35ħ state, i.e. the Yrast level in that for the Yrast level there is little single particle level crossing as the nucleus elongates whereas the 35ħ state based upon S3 has, after a few oscillations,

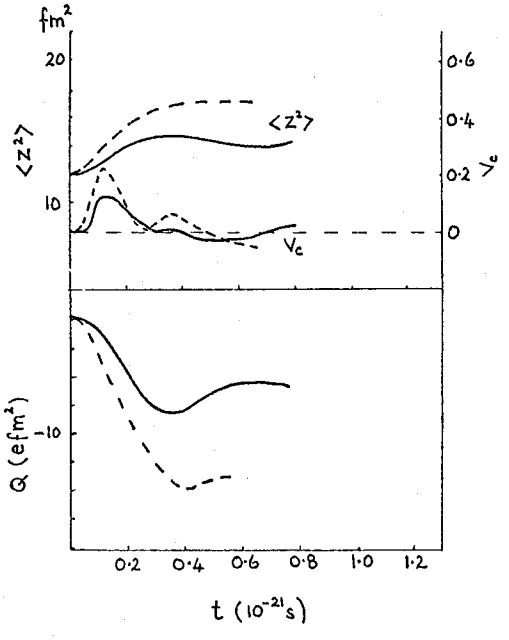

Figure 6

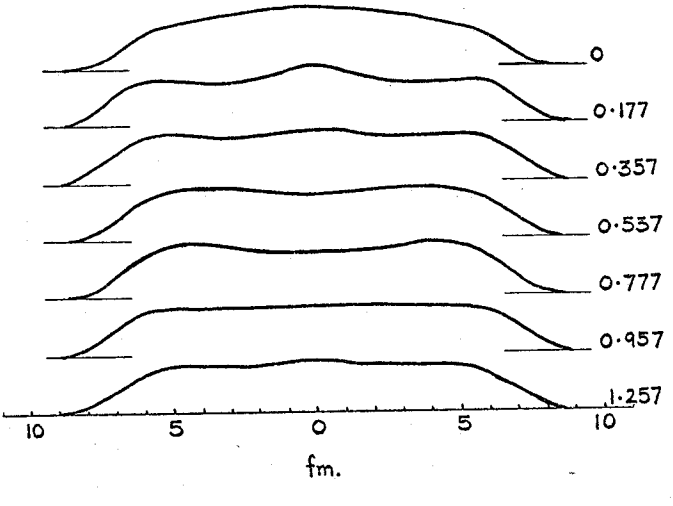

Figure 7

experienced considerable heating in the sense of much crossing of occupied and unoccupied single particle levels.

We next consider a 'model' rare earth nucleus ^{168}Gd in which we assume complete neutron-proton degeneracy and distribute the charge equally amongst all the nucleons. In these studies we initiated the TDHF evolution not only with rotations but also vibrations. Using eqtn.(7) the parameter α is chosen to give a certain amount of initial collective kinetic energy

$$E_{vib} = 4\alpha^2 \langle (z - z_0)^2 \rangle \hbar^2 A/2m \qquad (15)$$

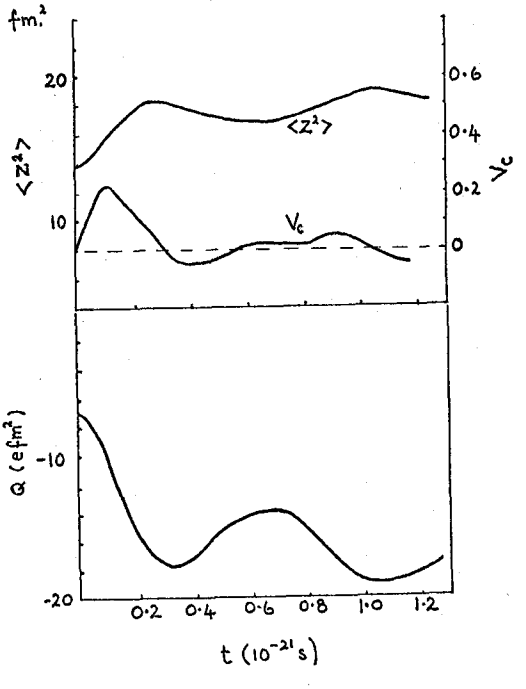

Figure 8

In figure 9 we plot the time evolution of the collective vibrational energy starting with an initial excitation of 162 MeV and in the absence any rotation. As with the rotational excitations we see a rapid damping of the collective motion. In figure 10 we plot the collective energy evolution of an initial configuration of 15$\hbar$ angular momentum (collective rotational energy 98.4 MeV) plus a vibrational excitation of 111.6 MeV. We see that the rotational mode damps first transferring its energy initially into the vibrational mode but that this then is also rapidly damped out. In figure 11 we plot the projected density profiles and while a pronounced dip in the central density does develop there is no indication of actual fission.

This rapid transfer of collective rotational energy into the vibration mode can be seen even more clearly in figure 12 where we have cranked up the angular momentum to 25$\hbar$ and reduced the initial E_{vib} to 20 MeV.

Finally we consider the role of the Coulomb force by doubling the effective charge on all the nucleons and adjusting the Skyrme parameters to give the same total binding energy as before. The rotational energy of the 15$\hbar$ state is raised from 98.4 MeV to 140 MeV and the density profiles are reproduced in figure 13. Again we see the development of a distinctive neck but still no fission.

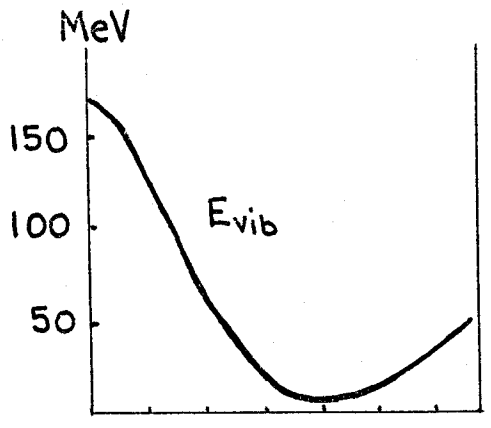

Figure 9

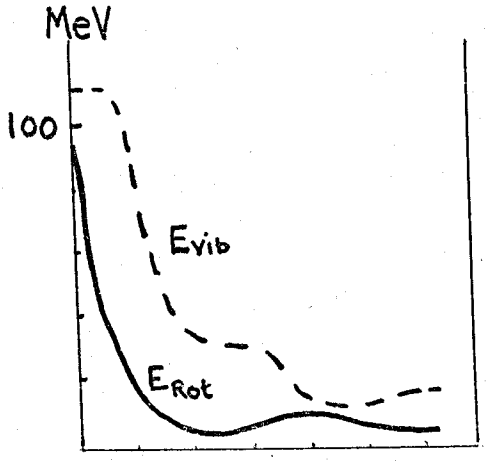

Figure 10

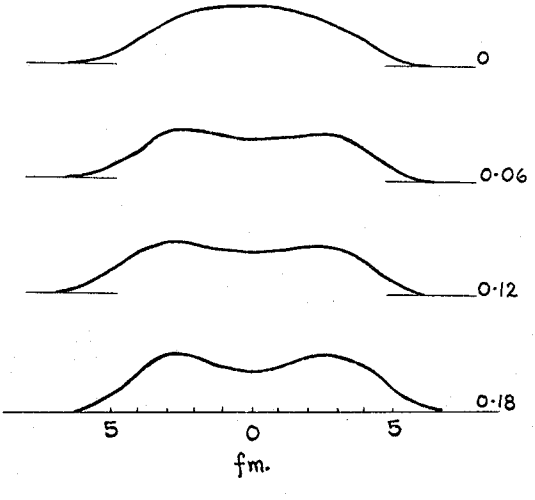

Figure 11

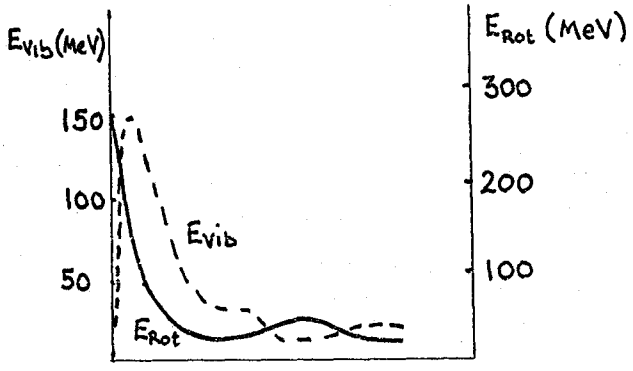

Figure 12

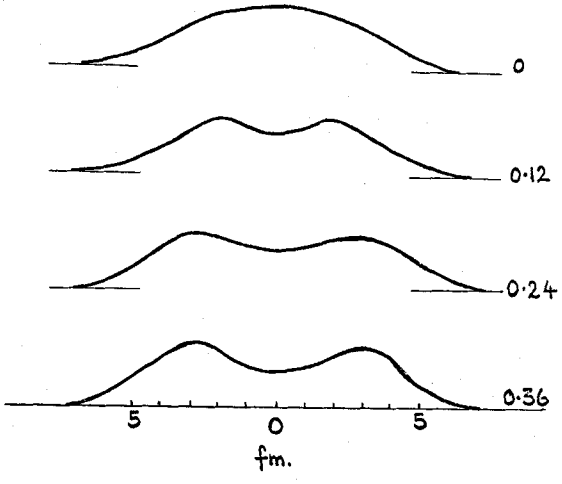

Figure 13

DISCUSSION

We have seen that within a TDHF description of collective nuclear motion any initial collective rotational energy is rapidly converted into stretching motion which can give rise to vibrations but these are always severely damped so that fission does not occur for modest initial excitations. If initially energy is put directly into the vibrational mode this is also severely damped. It is of course possible to initiate the evolution with sufficient collective excitation energy to guarantee fission but in our TDHF calculations at such excitation energies individual nucleons rapidly become unbound and the calculations terminate when these reach the edge of the mesh.

We are continuing these studies in two directions: We have seen that the vibrational mode most likely to lead to fission is heavily damped and the nucleus 'heats up' in the sense of there being many single particle level crossings. This one-body dissipation by the mean field can be avoided by going beyond TDHF to include collision terms which avoid the level crossings and should hence keep the nucleus 'cool' and its excitation energies in collective modes. Secondly, all the results quoted here are for collective excitations of H.F. configurations close to the ground state. We now intend to carry out a series of constrained static H.F. calculations for a range of deformations and cranked angular momenta in order to plot out the shape of the fission barrier. This will allow us to initiate the TDHF evolution close to the saddle point and hence hopefully to study the route to scission.

We are grateful to Dr. I.S. Grant for helpful discussions on the experimental background to heavy ion induced fission. One of us (J.N.) would like to express her appreciation to Dr. Nörenberg for his hospitality at G.S.I.